

Superconducting diode from flux biased Josephson junction arrays

Rafael Haenel^{1,2} and Oguzhan Can¹

¹*Department of Physics and Astronomy & Stewart Blusson Quantum Matter Institute, University of British Columbia, Vancouver BC, Canada V6T 1Z4*

²*Max Planck Institute for Solid State Research, 70569 Stuttgart, Germany*
(Dated: December 7, 2022)

We propose a realization of the superconducting diode effect in flux biased superconducting circuits of Josephson junctions. So far the observation of the superconducting diode effect has been limited to rather exotic material platforms. In theoretical proposals, it relied on a non-sinusoidal form of the current phase relation of Josephson junctions. Here, we show how the diode effect can be engineered in superconducting circuits without any such requirements. The only necessary ingredients are standard sinusoidal Josephson junctions and flux bias lines that are readily available in scalable industrial silicon-chip based superconducting design processes.

I. INTRODUCTION

The superconducting diode effect is present in a superconducting two-terminal device when it supports a larger critical current in forward direction than in backward direction. In the ideal limit of maximal imbalance, current applied in one direction is dissipationless (zero resistance), while it is always dissipative (resistive) in the opposite direction. This is a natural generalization of the semiconductor diode that is only weakly resistive in one direction and highly resistive in the opposite direction.

Recent interest in the superconducting diode effect has lead to a surge in experimental [1–11] and theoretical studies [12–24] including device proposals [25]. The common factor among them is reliance on a rather complicated material platform, precluding near-term commercial applications. The diode effect requires both inversion- and time-reversal symmetry breaking. Inversion can be absent in systems with spin-orbit coupling [10, 23], or it can be explicitly broken by twisting bilayers [7, 19, 26] or applying a current bias [27].

Two recent theoretical studies proposed a Josephson junction circuit realization of the superconducting diode effect, independent of an inversion symmetry breaking material platform [28, 29]. However, these proposals rely on high-harmonic content in the current phase relation of the junctions, i.e., a non-sinusoidal current phase relation. Inversion symmetry is broken by asymmetry of Josephson junctions in the circuit, which differ in their harmonic content.

In the present work, we propose a realization of the diode effect that removes all of the above requirements. It is based on a classical circuit of Josephson junctions with standard sinusoidal current phase relation. Junctions can in principle even be identical, and inversion symmetry is broken by the connectivity of the circuit. Time-reversal symmetry is broken by magnetic fluxes that can be applied using flux bias lines. The present diode implementation is agnostic to its underlying material platform and can be realized in industry standard Nb-Al processes based on scalable semiconductor technology.

This manuscript is organized as follows. In Sec. II A we introduce the simplest circuit that gives rise to a diode effect. The approach is based on a similar scheme of leveraging high-harmonics in the current phase relation as in [28, 29], with the key difference that *effective* high-harmonics are engineered by chaining identical junctions in series. We generalize this picture in Sec. II B, where we give an analytical form for junction and flux parameters that achieve the most optimal diode for this geometry. In Sec. III we discuss effects of parasitic resistors, capacitors, and inductors. We conclude with a summary in Sec. IV.

II. THE DIODE EFFECT IN A SUPERCONDUCTING JOSEPHSON CIRCUIT

A. Minimal circuit

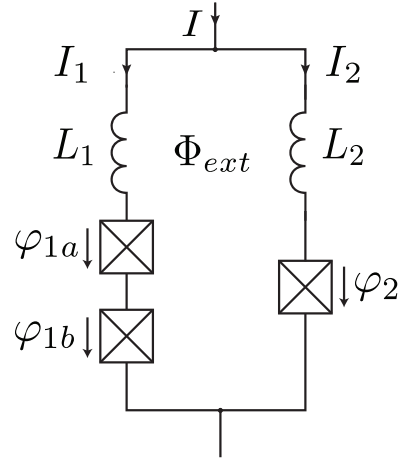


FIG. 1. Superconducting circuit consisting of two inductive arms with one and two Josephson junctions in series, respectively. An external flux Φ_{ext} may thread the superconducting loop. Here, the inductors L_1, L_2 represent the geometric inductance of the superconducting wires.

We consider the superconducting circuit depicted in

Fig. 1 consisting of two arms of Josephson junctions (JJ). The first arm consists of two junctions across which the superconducting phase jumps by φ_{1a} , φ_{1b} , respectively. The second arm consists of single Josephson junction with phase difference φ_2 . The parasitic inductance of the wires is modeled by the lumped inductors L_1, L_2 . This circuit has been previously introduced in the context of second harmonic generation, where it is known as the Superconducting Nonlinear Asymmetric Inductive Element (SNAIL) [30].

The supercurrents in both arms of the SNAIL are determined by the Josephson relations

$$I_1 = I_c^{(1a)} \sin \varphi_{1a} = I_c^{(1b)} \sin \varphi_{1b} \quad (1)$$

$$I_2 = I_c^{(2)} \sin \varphi_2. \quad (2)$$

We will be interested in the case of identical junction in the first arm, i.e., $I_c^{(1a)} = I_c^{(1b)}$. Here, the phases across the junctions are equal, $\varphi_{1a} = \varphi_{1b} \equiv \varphi_1$. Continuity of the phase along the superconducting loop then yields the phase quantization condition

$$2\varphi_1 - \varphi_2 + 2\pi n = 2\pi\Phi/\Phi_0 \quad (3)$$

where Φ is the total flux threading the junction and $\Phi_0 = h/2e$ is the superconducting flux quantum.

For small circuits the geometric inductance can be neglected, $L_a, L_b \rightarrow 0$. Then, flux through the loop is solely determined by the external flux, i.e., $\Phi = \Phi_{ext}$. The total current is

$$I(\varphi) = I_1 + I_2 = I_c^{(1)} \sin \varphi_1 + I_c^{(2)} \sin(2\varphi_1 - \varphi_{ext}) \quad (4)$$

where we have defined $\varphi_{ext} = 2\pi\Phi_{ext}/\Phi_0$.

The critical current in positive and negative direction are defined as

$$\begin{aligned} I_c^+ &\equiv \max_{\varphi} I(\varphi) \\ I_c^- &\equiv \left| \min_{\varphi} I(\varphi) \right| \end{aligned} \quad (5)$$

where we note that I_c^+ and I_c^- are positive quantities. Importantly, for $\varphi_{ext}/2\pi \notin \mathbf{Z}$, i.e., when φ_{ext} is a non-trivial phase, one generally has

$$I_c^+ \neq I_c^-, \quad (6)$$

i.e., the forward and backward applied critical currents are imbalanced. This constitutes the superconducting diode effect. The degree of imbalance between these two critical current values is quantified by the superconducting diode efficiency

$$\eta = \frac{|I_c^+ - I_c^-|}{I_c^+ + I_c^-}, \quad (7)$$

which is a positive number and $\eta < 1$. We find the maximum efficiency of $\eta = 1/3$ for the two-arm geometry in Fig. 1 when $I_c^{(2)} = I_c^{(1)}/2$ and $\Phi_{ext} = \Phi_0/4$.

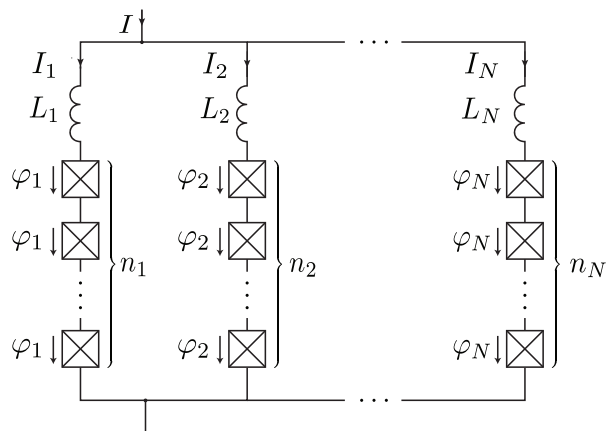


FIG. 2. Generalized Josephson interferometer consisting of N arms with current I_k and n_k identical Josephson junctions with critical current $I_c^{(k)}$ that each experience a superconducting phase drop φ_k . Geometrical inductances have been lumped into the elements L_k . A magnetic flux $\Phi_{k,l}$ may be threaded between arms k and l .

B. N -arm interferometers and the ideal diode limit

Next we consider a N -ladder of JJ arrays which we enumerate by $k = 1, \dots, N$ with n_k consecutive junctions forming each arm k and flux $\Phi_{k,l}$ enclosed between the arms k and l . By phase continuity, the Josephson phase for a single junction in arm k in terms of the phase variable φ_1 is given by

$$\varphi_k = \frac{n_1\varphi_1 - \frac{2\pi}{\Phi_0}\Phi_{1,k}^{ext} + 2\pi n}{n_k} \quad (8)$$

in the limit of zero inductance.

We assume the zero-vortex state $n = 0$ and define $\phi_k^{ext} = \frac{1}{n_k} \frac{2\pi}{\Phi_0} \Phi_{1,k}^{ext}$. Then, the total current is

$$I(\varphi_1) = \sum_k I_k = \sum_{k=1}^N I_c^{(k)} \sin\left(\frac{n_1}{n_k}\varphi_1 - \phi_k^{ext}\right). \quad (9)$$

If the integer coefficients n_k are chosen in such a way that

$$n_1/n_k = k, \quad (10)$$

Eq. (9) represents a Fourier series that allows for engineering of arbitrary current phase relations. One such set of integers is given by $n_k = N! / [\text{floor}(N/2)! k!]$. For an efficient diode layout, one should however reduce this set by its greatest common denominator, $GCD(\{n_k\})$.

The Fourier series is fully specified by the individual magnetic flux parameters ϕ_k^{ext} and critical currents $I_c^{(k)}$. The fluxes are easily tuned via flux bias lines and critical currents are determined by the junction area in the fabrication design.

We are now left to discuss the problem of finding the set of parameters that yield the greatest diode efficiency

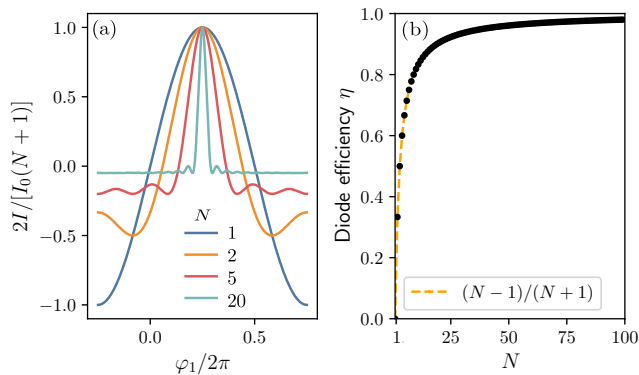


FIG. 3. (a) Current phase relation for number of interferometer arms $N = 1, 2, 5, 20$ and (b) diode efficiency as a function of N that is given by $\eta = (N - 1)/(N + 1)$.

η . Let us propose the particular choice

$$I_c^{(k)} = I_0 \frac{N + 1 - k}{N} \quad (11)$$

$$\phi_k^{ext} = (k - 1)\pi/2 \quad (12)$$

This yields the following analytical expression for the total current of the interferometer:

$$\begin{aligned} I(\varphi_1)/I_0 &= \sum_{k=1}^N \frac{N + 1 - k}{N} \sin(k\varphi_1 + (1 - k)\pi/2) \\ &= \frac{\cos((N + 1)(\varphi_1 - \pi/2)) - 1}{2N(\sin \varphi_1 - 1)} - \frac{N + 1}{2N} \end{aligned} \quad (13)$$

A plot of Eq. (13) for various N is shown in Fig. 3(a). As N is increased, the function develops a narrow peak of height $I/I_0 = (N + 1)/2$ at $\varphi_1 = \pi/2$ over a seemingly flat background at $I/I_0 = (N + 1)/2N$, yielding a significant imbalance of critical currents with diode efficiency

$$\eta = \frac{N - 1}{N + 1} \quad (14)$$

that approaches unity in the large- N limit. In fact, for $N \rightarrow \infty$, the current-phase relation approaches a series of δ -functions centered at $2\pi(n + 1/4)$ and shifted by a constant current $-I_0/2$, according to

$$\lim_{N \rightarrow \infty} I/I_0 = \pi \sum_k \delta(\varphi_1 - \pi/2 + 2\pi k) - \frac{1}{2}. \quad (15)$$

While the flux and critical current parameters defined in Eqs. (11-12) yield an ideal diode in the large- N limit, they likely also constitute the fastest converging series. For small $N \leq 5$, where the parameter space is still amenable to numerical optimization, we have numerically confirmed that it represents the optimal solution.

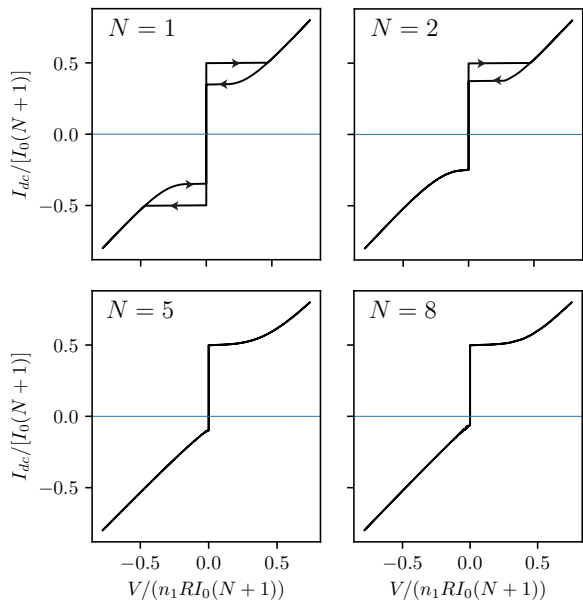


FIG. 4. I - V curves computed within RSJ model for $\beta = 0.6\sqrt{n_1}$ and $N = 1, 2, 5, 20$

III. PARASITIC COMPONENTS

A. IV-characteristic

We now consider a resistively and capacitively shunted junction (RCSJ) model where each junction on arm k in Fig. 2 is shunted by an internal capacitor C_k and resistor R_k . For an external dc current bias $I_{dc}^{(k)}$ in arm k the equation of motion is given by

$$I_{dc}^{(k)} = \frac{\Phi_0}{2\pi} \frac{\dot{\varphi}_k}{R_k} + \frac{\Phi_0}{2\pi} C_k \ddot{\varphi}_k + I_c^{(k)} \sin \varphi_k \quad (16)$$

We assume that every junction is identical for a given arm and current conservation implies that φ_k is the same for every junction. Using the phase continuity condition (8) and adding all currents one can show that the system is governed by a single differential equation

$$I_{dc}/I_0 = \frac{d^2\varphi_1}{d\tau^2} + \beta \frac{d\varphi_1}{d\tau} + I(\varphi_1)/I_0, \quad (17)$$

where $I_{dc} = \sum_k I_{dc}^{(k)}$ is the total, experimentally applied current bias. We have also defined the dimensionless parameters $\tau = \omega_J t$, $\beta = (\omega_J R_{\text{eff}} C_{\text{eff}})^{-1}$, $\omega_J = \sqrt{\frac{2e}{\hbar} \frac{I_0}{C_{\text{eff}}}}$ and the effective resistance and capacitance parameters

$$R_{\text{eff}} = \left(\sum_{k=1}^N \frac{n_1}{R_k n_k} + \frac{n_1}{R_{\text{ext}}} \right)^{-1} \quad (18)$$

$$C_{\text{eff}} = \sum_{k=1}^N \frac{n_1 C_k}{n_k} + n_1 C_{\text{ext}}. \quad (19)$$

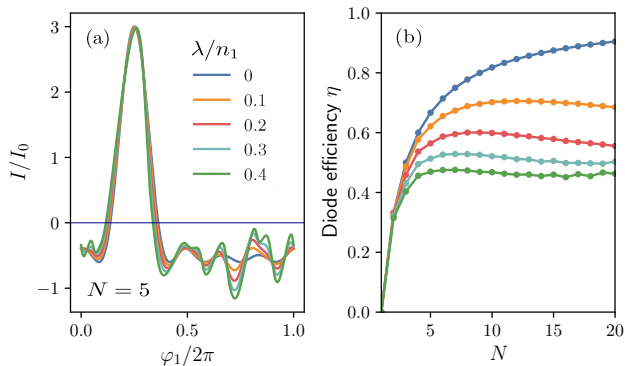


FIG. 5. Current phase relation (a) for the exemplary case $N = 5$ and (b) diode efficiency as a function of N for varied strength of the inductance parameter λ/n_1 . The geometrical inductance distorts the current-phase relation and diminishes the diode efficiency η .

N	η	N_J	n_k	$\Phi_{k,k+1}/\Phi_0$	$I_c^{(k)}N/I_0$
2	1/3	3	2 1	1/4	2 1
3	1/2	11	6 3 2	3/4 1/4	3 2 1
4	3/5	25	12 6 4 3	3/2 1/2 1/4	4 3 2 1
5	2/3	137	60 30 20 15 12	7.5 5/2 5/4 3/4	5 4 3 2 1

TABLE I. Optimal parameters for superconducting diode circuits with N arms. $N_J = \sum_k n_k$ is the total number of Josephson junctions required and $\Phi_{k,k+1}$ is the magnetic flux threaded between arms k and $k+1$.

R_k and C_k will depend on the geometries of individual junctions. For better tunability, one may shunt the entire device with an additional resistor R_{ext} and a capacitor C_{ext} . The voltage across each arm is given by $V = n_1 \frac{\Phi_0}{2\pi} \dot{\varphi}_1$. In the limit where $R_{ext} \ll R_k$ and $C_{ext} \gg C_k$, dynamics is independent of internal resistances and capacitances of the junctions, where we find $R_{eff} \approx R_{ext}/n_1$ and $C_{eff} \approx n_1 C_{ext}$. In this limit, β defined just below 17 scales as $\beta \approx \sqrt{N!}$ where $\tilde{\omega} = \sqrt{\frac{2e}{\hbar} \frac{I_0}{C_{ext}}}$ and n_1 is the number of junctions on arm $k=1$ which depends on N as $n_k \approx N!$ in the large- N limit.

We numerically solve the differential Eq. (17) for voltage as a function of external current I_{dc} . The resulting I - V -curves are shown in Fig. 4 for various N and $\beta = 0.6\sqrt{n_1}$. For $N > 1$, the critical currents become imbalanced. The I - V -curves display a well-known hysteretic behavior which, however, can be suppressed for large N , i.e., when β is sufficiently large.

B. Finite inductance

In the case of finite geometric inductance, $L_k > 0$, the flux through the superconducting loops is no longer defined just by the external flux. Instead, Eq. (8) must be modified to also include the contribution of the induced

flux,

$$\varphi_k = \frac{1}{n_k} \frac{2\pi}{\Phi_0} (\Phi_{1,k}^{ext} + L_1 I_1 - L_k I_k). \quad (20)$$

Now, Eq. (9) must be solved self-consistently, since a change in current implies a change in φ_k , which again induces a change in the I_k . For sufficiently large inductances, the induced fluxes will develop hysteretic behavior in the externally applied flux.

Since the geometrical inductances are expected to be roughly equal for each arm, we parametrize them by a single dimensionless parameter $2\pi L_i/\Phi_0 \equiv \lambda$. In Fig. 5, we show the results of the self-consistent calculation for various λ , small enough that the diode is still in the non-hysteretic regime. The inductance can be seen to distort the current phase relation and yields an overall decrease in diode efficiency. Assuming that the λ roughly scales with the maximum number of junctions in a branch n_1 , this efficiency decrease is more pronounced at large N .

IV. DISCUSSION AND SUMMARY

We have proposed a superconducting diode circuit element that requires only conventional Josephson junctions and flux bias loops which can be fabricated utilizing existing integrated circuit technology.

A Josephson interferometer will exhibit the superconducting diode effect if current arms carry different harmonics $\sin n\varphi$ of the current phase relation and if these harmonics are phase-shifted with respect to each other.

We have shown that higher harmonics can effectively be generated in generalized SNAIL geometries when multiple conventional Josephson junctions are connected in series. Flux biases in the loops are crucial for generating the phase differences, which we have optimized for diode efficiency. Note that polarity of the superconducting diode can be switched by reversal of all fluxes, i.e., by setting $\varphi_{k,ext} \rightarrow -\varphi_{k,ext}$ in Eq. (12). We have also considered the effects of geometric inductance, which lead to an overall decrease in diode efficiency.

We work in the limit $E_J \gg E_C$ where charging energy is $E_c = e^2/2C_J$. Here, fluctuations in the phase variable φ are suppressed. Therefore φ can be treated as a classical variable, justifying the use of RSJ model in Eq. (4).

Table I summarizes the various optical circuit parameters for different N , along with the resulting diode efficiency in the non-inductive case. Circuits with more than a few arms are likely mostly of academic interest, as the total number of required junctions scales exponentially in N , even though more than 10^6 Josephson junctions and on the order of 10^5 flux biases have been integrated on a single chip [31, 32]. Nevertheless, for reasonably small N , our proposed diode device could be promising for practical use.

Note added. During preparation of this manuscript, we learned about a related experimental work [33] that has

fabricated and measured the circuit geometry in Fig. 1 for the simplest case, $N = 2$. In their setup, three identical junctions were used, limiting the theoretically achievable efficiency to $\eta = 0.28$ instead of $1/3$, which was measured to be $\eta \sim 0.12$ in the experiment.

V. ACKNOWLEDGMENTS

We thank Marcel Franz, Shannon Egan, and Joe Salfi for enlightening discussions. This work was supported by

NSERC, the Max Planck-UBC-UTokyo Centre for Quantum Materials and the Canada First Research Excellence Fund, Quantum Materials and Future Technologies Program.

-
- [1] Ryohei Wakatsuki, Yu Saito, Shintaro Hoshino, Yuki M. Itahashi, Toshiya Ideue, Motohiko Ezawa, Yoshihiro Iwasa, and Naoto Nagaosa, “Nonreciprocal charge transport in noncentrosymmetric superconductors,” *Science Advances* **3**, e1602390 (2017), <https://www.science.org/doi/pdf/10.1126/sciadv.1602390>.
- [2] Kenji Yasuda, Hironori Yasuda, Tian Liang, Ryutaro Yoshimi, Atsushi Tsukazaki, Kei S. Takahashi, Naoto Nagaosa, Masashi Kawasaki, and Yoshinori Tokura, “Nonreciprocal charge transport at topological insulator/superconductor interface,” *Nature Communications* **10**, 2734 (2019).
- [3] Fuyuki Ando, Yuta Miyasaka, Tian Li, Jun Ishizuka, Tomonori Arakawa, Yoichi Shiotani, Takahiro Moriyama, Youichi Yanase, and Teruo Ono, “Observation of superconducting diode effect,” *Nature* **584**, 373–376 (2020).
- [4] Banabir Pal, Anirban Chakraborty, Pranava K. Sivakumar, Margarita Davydova, Ajesh K. Gopi, Avanindra K. Pandeya, Jonas A. Krieger, Yang Zhang, Mihir Date, Sailong Ju, Noah Yuan, Niels B. M. Schröter, Liang Fu, and Stuart S. P. Parkin, “Josephson diode effect from cooper pair momentum in a topological semimetal,” (2021), [10.48550/ARXIV.2112.11285](https://arxiv.org/abs/2112.11285).
- [5] Yang-Yang Lyu, Ji Jiang, Yong-Lei Wang, Zhi-Li Xiao, Sining Dong, Qing-Hu Chen, Milorad V. Milošević, Huabing Wang, Ralu Divan, John E. Pearson, Peiheng Wu, Francois M. Peeters, and Wai-Kwong Kwok, “Superconducting diode effect via conformal-mapped nanoholes,” *Nature Communications* **12**, 2703 (2021).
- [6] Jeacheol Shin, Suhan Son, Jonginn Yun, Giung Park, Kaixuan Zhang, Young Jae Shin, Je-Geun Park, and Dohun Kim, “Magnetic proximity-induced superconducting diode effect and infinite magnetoresistance in van der waals heterostructure,” (2021).
- [7] Jiang-Xiazi Lin, Phum Siriviboon, Harley D. Scammell, Song Liu, Daniel Rhodes, K. Watanabe, T. Taniguchi, James Hone, Mathias S. Scheurer, and J. I. A. Li, “Zero-field superconducting diode effect in small-twist-angle trilayer graphene,” *Nature Physics* **18**, 1221–1227 (2022).
- [8] Ji Jiang, M.V. Milošević, Yong-Lei Wang, Zhi-Li Xiao, F.M. Peeters, and Qing-Hu Chen, “Field-free superconducting diode in a magnetically nanostructured superconductor,” *Phys. Rev. Applied* **18**, 034064 (2022).
- [9] Lorenz Bauriedl, Christian Bäuml, Lorenz Fuchs, Christian Baumgartner, Nicolas Paulik, Jonas M. Bauer, Kai-Qiang Lin, John M. Lupton, Takashi Taniguchi, Kenji Watanabe, Christoph Strunk, and Nicola Paradiso, “Supercurrent diode effect and magnetochiral anisotropy in few-layer nbse2,” *Nature Communications* **13**, 4266 (2022).
- [10] Christian Baumgartner, Lorenz Fuchs, Andreas Costa, Simon Reinhardt, Sergei Gronin, Geoffrey C. Gardner, Tyler Lindemann, Michael J. Manfra, Paulo E. Faria Junior, Denis Kochan, Jaroslav Fabian, Nicola Paradiso, and Christoph Strunk, “Supercurrent rectification and magnetochiral effects in symmetric josephson junctions,” *Nature Nanotechnology* **17**, 39–44 (2022).
- [11] Heng Wu, Yaojia Wang, Yuanfeng Xu, Pranava K. Sivakumar, Chris Pasco, Ulderico Filippozzi, Stuart S. P. Parkin, Yu-Jia Zeng, Tyrel McQueen, and Mazhar N. Ali, “The field-free josephson diode in a van der waals heterostructure,” *Nature* **604**, 653–656 (2022).
- [12] Shintaro Hoshino, Ryohei Wakatsuki, Keita Hamamoto, and Naoto Nagaosa, “Nonreciprocal charge transport in two-dimensional noncentrosymmetric superconductors,” *Phys. Rev. B* **98**, 054510 (2018).
- [13] Kou Misaki and Naoto Nagaosa, “Theory of the nonreciprocal josephson effect,” *Phys. Rev. B* **103**, 245302 (2021).
- [14] A. A. Kopasov, A. G. Kutlin, and A. S. Mel’nikov, “Geometry controlled superconducting diode and anomalous josephson effect triggered by the topological phase transition in curved proximitized nanowires,” *Phys. Rev. B* **103**, 144520 (2021).
- [15] Akito Daido, Yuhei Ikeda, and Youichi Yanase, “Intrinsic superconducting diode effect,” *Phys. Rev. Lett.* **128**, 037001 (2022).
- [16] Bastian Zinkl, Keita Hamamoto, and Manfred Sigrist, “Symmetry conditions for the superconducting diode effect in chiral superconductors,” *Phys. Rev. Research* **4**, 033167 (2022).
- [17] Margarita Davydova, Saranesh Prembabu, and Liang Fu, “Universal josephson diode effect,” *Science Advances* **8**, eabo0309 (2022), <https://www.science.org/doi/pdf/10.1126/sciadv.abo0309>.
- [18] Klaus Halterman, Mohammad Alidoust, Ross Smith, and Spencer Starr, “Supercurrent diode effect, spin torques, and robust zero-energy peak in planar half-metallic trilayers,” *Phys. Rev. B* **105**, 104508 (2022).
- [19] Harley D Scammell, J I A Li, and Mathias S Scheurer, “Theory of zero-field superconducting diode effect in twisted trilayer graphene,” *2D Materials* **9**, 025027 (2022).

- [20] Noah F. Q. Yuan and Liang Fu, “Supercurrent diode effect and finite-momentum superconductors,” *Proceedings of the National Academy of Sciences* **119**, e2119548119 (2022), <https://www.pnas.org/doi/pdf/10.1073/pnas.2119548119>.
- [21] Yi Zhang, Yuhao Gu, Pengfei Li, Jiangping Hu, and Kun Jiang, “General theory of josephson diodes,” *Phys. Rev. X* **12**, 041013 (2022).
- [22] Baoxing Zhai, Bohao Li, Yao Wen, Fengcheng Wu, and Jun He, “Prediction of ferroelectric superconductors with reversible superconducting diode effect,” *Phys. Rev. B* **106**, L140505 (2022).
- [23] S. Ilić and F. S. Bergeret, “Theory of the supercurrent diode effect in rashba superconductors with arbitrary disorder,” *Phys. Rev. Lett.* **128**, 177001 (2022).
- [24] Yukio Tanaka, Bo Lu, and Naoto Nagaosa, “Theory of diode effect in d-wave superconductor junctions on the surface of topological insulator,” (2022), [10.48550/ARXIV.2205.13177](https://arxiv.org/abs/2205.13177).
- [25] Jiangping Hu, Congjun Wu, and Xi Dai, “Proposed design of a josephson diode,” *Phys. Rev. Lett.* **99**, 067004 (2007).
- [26] Sanat Ghosh, Vilas Patil, Amit Basu, Kuldeep, Digambar A. Jangade, Ruta Kulkarni, A. Thamizhavel, and Mandar M. Deshmukh, “High-temperature superconducting diode,” (2022).
- [27] John Chiles, Ethan G. Arnault, Chun-Chia Chen, Trevyn F. Q. Larson, Lingfei Zhao, Kenji Watanabe, Takashi Taniguchi, François Amet, and Gleb Finkelstein, “Non-reciprocal supercurrents in a field-free graphene josephson triode,” (2022).
- [28] Ya. V. Fominov and D. S. Mikhailov, “Asymmetric higher-harmonic squid as a josephson diode,” *Phys. Rev. B* **106**, 134514 (2022).
- [29] Rubén Seoane Souto, Martin Leijnse, and Constantin Schrader, “The josephson diode effect in supercurrent interferometers,” (2022), [10.48550/ARXIV.2205.04469](https://arxiv.org/abs/2205.04469).
- [30] N. E. Frattini, U. Vool, S. Shankar, A. Narla, K. M. Sliwa, and M. H. Devoret, “3-wave mixing josephson dipole element,” *Applied Physics Letters* **110**, 222603 (2017), <https://doi.org/10.1063/1.4984142>.
- [31] R. Harris, J. Johansson, A. J. Berkley, M. W. Johnson, T. Lanting, Siyuan Han, P. Bunyk, E. Ladizinsky, T. Oh, I. Perminov, E. Tolkacheva, S. Uchaikin, E. M. Chapple, C. Enderud, C. Rich, M. Thom, J. Wang, B. Wilson, and G. Rose, “Experimental demonstration of a robust and scalable flux qubit,” *Phys. Rev. B* **81**, 134510 (2010).
- [32] Kelly Boothby, Colin Enderud, Trevor Lanting, Reza Molavi, Nicholas Tsai, Mark H. Volkmann, Fabio Altomare, Mohammad H. Amin, Michael Babcock, Andrew J. Berkley, Catia Baron Aznar, Martin Boschnak, Holly Christiani, Sara Ejtemaee, Bram Evert, Matthew Gullen, Markus Hager, Richard Harris, Emile Hoskinson, Jeremy P. Hilton, Kais Jooya, Ann Huang, Mark W. Johnson, Andrew D. King, Eric Ladizinsky, Ryan Li, Allison MacDonald, Teresa Medina Fernandez, Richard Neufeld, Mana Norouzpour, Travis Oh, Isil Ozfidan, Paul Paddon, Ilya Perminov, Gabriel Poulin-Lamarre, Thomas Prescott, Jack Raymond, Mauricio Reis, Chris Rich, Aidan Roy, Hossein Sadeghi Esfahani, Yuki Sato, Ben Sheldan, Anatoly Smirnov, Loren J. Swenson, Jed Whittaker, Jason Yao, Alexander Yarovoy, and Paul I. Bunyk, “Architectural considerations in the design of a third-generation superconducting quantum annealing processor,” (2021).
- [33] Mohit Gupta, Gino V. Graziano, Mihir Pendharkar, Jason T. Dong, Connor P. Dempsey, Chris Palmstrøm, and Vlad S. Pribiag, “Superconducting diode effect in a three-terminal josephson device,” (2022)